Methods for Evaluating DC Arc Incident Energy in PV Systems

Preprint

William Sekulic,[1] Albert Marroquin,[2] and Peter McNutt[1]

1 National Renewable Energy Laboratory
2 ETAP - Operation Technology, Inc.

Presented at the IEEE Electrical Safety Workshop
March 8-12, 2021

NREL is a national laboratory of the U.S. Department of Energy
Office of Energy Efficiency & Renewable Energy
Operated by the Alliance for Sustainable Energy, LLC

This report is available at no cost from the National Renewable Energy Laboratory (NREL) at www.nrel.gov/publications.

Contract No. DE-AC36-08GO28308

Conference Paper
NREL/CP-5K00-78331
August 2021

Methods for Evaluating DC Arc Incident Energy in PV Systems

Preprint

William Sekulic,[1] Albert Marroquin,[2] and Peter McNutt[1]

1 National Renewable Energy Laboratory
2 ETAP - Operation Technology, Inc.

Suggested Citation
Sekulic, William, Albert Marroquin, and Peter McNutt. 2021. *Methods for Evaluating DC Arc Incident Energy in PV Systems Preprint*. Golden, CO: National Renewable Energy Laboratory. NREL/CP-5K00-78331. https://www.nrel.gov/docs/fy21osti/78331.pdf.

NREL is a national laboratory of the U.S. Department of Energy
Office of Energy Efficiency & Renewable Energy
Operated by the Alliance for Sustainable Energy, LLC

This report is available at no cost from the National Renewable Energy Laboratory (NREL) at www.nrel.gov/publications.

Contract No. DE-AC36-08GO28308

Conference Paper
NREL/CP-5K00-78331
August 2021

National Renewable Energy Laboratory
15013 Denver West Parkway
Golden, CO 80401
303-275-3000 • www.nrel.gov

NOTICE

This work was authored by the National Renewable Energy Laboratory, operated by Alliance for Sustainable Energy, LLC, for the U.S. Department of Energy (DOE) under Contract No. DE-AC36-08GO28308. Funding provided by the U.S. Department of Energy Office of Energy Efficiency and Renewable Energy Solar Energy Technologies Office. The views expressed herein do not necessarily represent the views of the DOE or the U.S. Government. The U.S. Government retains and the publisher, by accepting the article for publication, acknowledges that the U.S. Government retains a nonexclusive, paid-up, irrevocable, worldwide license to publish or reproduce the published form of this work, or allow others to do so, for U.S. Government purposes.

Cover Photos by Dennis Schroeder: (clockwise, left to right) NREL 51934, NREL 45897, NREL 42160, NREL 45891, NREL 48097, NREL 46526.

Methods for Evaluating DC Arc Incident Energy in PV Systems

Paper No. ESW2021-05

William Sekulic
Member, IEEE
NREL
Golden, Co 80401
bill.sekulic@nrel.gov

Albert Marroquin
Senior Member
ETAP
Irvine, CA 92618
albert.marroquin@etap.com

Peter McNutt
Senior Member
NREL
Golden, Co 80401
peter.mcnutt@nrel.gov

Abstract – Renewable energy systems continue to be one of the fastest growing segments of the energy industry. This paper focuses on the understanding of how photovoltaic (PV) technology behaves under dc arc conditions. Emphasis is placed on the electrical safety aspect of DC arc flash incident energy evaluation. Because of the fast proliferation of PV systems and the lack of formal equivalent calculation guidelines such as IEEE 1584 for AC systems, it has been necessary to rely on different equations and models presented by various researchers over the last few years. This paper discusses the behavior of PV systems under arc conditions and presents the results of available methods to estimate the dc arc flash incident energy. This paper provides a comparative analysis of a proposed arc-flash incident energy calculation method against different laboratory tests including those performed for this paper at the National Renewable Energy Laboratory (NREL). Detailed explanations are provided regarding the effect of PV module I-V and P-V curves under arcing conditions. Examples of the application of the proposed calculation method to the test measurements are included.

Index Terms — DC Arc Flash, DC Arc, Arc Resistance, dc arc flash methods, Voc – Open circuit voltage; dc Isc–short circuit current; MPPT–maximum power point, IV Curve–voltage and current curve; PV – Photovoltaic

I. INTRODUCTION

Global energy demand is projected to double from 13 TW to 28TW by the middle of the century. The need for cleaner energy has caused a proliferation of PV system installations. Just like any other electrical equipment, PV systems present electrical hazards. Several researchers over the years have recognized that it is extremely important to accurately quantify the hazard of dc PV arc flash incident energy. The purpose of this paper is to discuss how the dc arc flash incident energy calculation methods compare against the authors' laboratory tests and also against tests performed by other organizations for the end purpose of providing a more cohesive approach for evaluating hazards related with photovoltaic systems.

The goal of an arc flash incident energy (I.E.) calculation is to help in the selection of the appropriate personal protective equipment for the task. However, if the I.E. is overestimated, it may cause workers exposed to the hazard to overly protect (i.e. wear heavy PPE) which can introduce other hazards. Current guidance on protection of workers from electrical hazards including arc flash are provided in National Fire Protection Association (NFPA) 70E [1], a US national consensus standard, which works together with NFPA 70 (the US National Electric Code or NEC) to protect workers from arc flash hazards. The NEC mandates marking of electrical equipment, such as switchboards, switchgear, panelboards, industrial control panels, meter socket enclosures, and motor control centers, to warn qualified persons of potential electric arc flash hazards. The NEC also provides requirements for PV systems safety in article 690 [2].

Much of the current focus of NFPA 70E for arc calculations is for AC systems without inherent limitations to supplied power or energy, aside from maximum fault currents of upstream transformers or switchgear. For DC arcs in PV systems on the other hand, the dynamics of PV systems' short-circuit current and power vs voltage characteristic along with inherent power limits based on available irradiance makes them a special class of equipment which cannot be modeled accurately by using simplified methods such as the maximum power method found in NFPA 70E Annex D.5.

The aim of this paper is to discuss the basic principles of PV systems such as their current-voltage (I-V) and power-voltage (P-V) characteristic curves and explain how they should be used along with dc arc equations to estimate the arc voltage and resistance for DC incident energy calculations. The proposed method combines the PV and arc characteristics to accomplish this. The method was validated using comparisons against various field tests employing real PV systems, and compared with existing incident energy models.

II. REGULATORY REQUIREMENTS

Electrical arc flash has been identified by OSHA as a serious hazard requiring mitigation. As stated in OSHA article 1910.335: "to warn and protect employees from hazards which could cause injury due to electric shock, burns or failure of electric equipment parts" [3]. OSHA requires employers to protect workers from electrical hazards including arc flash. NFPA 70E is a national consensus standard with detailed information to help individuals comply with OSHA on how to protect workers from arc flash hazards. The NEC mandates marking of electrical equipment, such as switchboards, switchgear, panelboards, industrial control panels, meter socket enclosures, and motor control centers, anything likely to require examination, adjustment, servicing, or maintenance while energized. The equipment shall be field, or factory marked to warn qualified persons of potential electric arc flash hazards. The NEC also provides requirements for electrical systems in article 110.16 and PV systems in article 690.

III. Modelling

One of the most important aspect of the methods used to calculate the dc arc-flash incident energy for PV systems is the calculation of the arc current from the panel I-V characteristics. To calculate the current, we need to understand how PV modules connected into PV arrays work.

A PV array can be made up of several modules in series and parallel. In most cases the modules are of the same type (i.e. same manufacturer and model). The most fundamental step is to select the individual PV module ratings including P-V and I-V curves. The array is just a combination of the modules.

Current versus voltage (I-V) characteristics of the PV module can be defined in sunlight and under dark conditions as shown in Fig. 1. In the first quadrant, the top left of the I-V curve at zero voltage is called the short circuit current. This is the current measured with the output terminals shorted (zero voltage). The bottom right of the curve at zero current is called the open-circuit voltage. This is the voltage measured with the output terminals open (zero current).

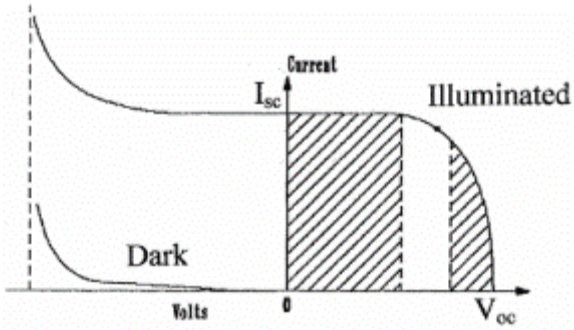

Fig. 1-I-V Curve under Illumination and Dark Conditions

If a voltage is externally applied in the reverse direction, (e.g., during a system fault transient), the current remains flat and the power is absorbed by the cell. However, beyond a certain negative voltage, the junction diode breaks down, and the current rises to a high value. In the dark, the current is zero for voltage up to the breakdown voltage which is the same as in the illuminated condition. This paper does not intend to discuss dc arc-flash hazard conditions during nighttime or low illumination conditions, but hazards could still exist if external negative voltage is applied to the panels [4].

There are several methods to model the I-V curves for a PV module. Since the dc arc in the PV system is expected to produce an arc voltage which is on the far left of the maximum power voltage (V_{mp}), then a linear representation of the I-V curve between the 0 volts and V_{mp} is often sufficient to estimate the operating voltage of the arc to enough accuracy. Equations (1) and (2) below can be used to estimate a linear set of points for the I-V curves with only a few voltage steps. Fig. 2 shows a set of I-V of curves developed based on this approach.

$$V_{oc}(T_a, G) = V_b\left[1 + \frac{\beta_{Voc}}{100} \times (T_a - T_b) + \delta_{Voc} \times \ln\left(\frac{G}{G_b}\right)\right] \quad (1)$$

$$I_{sc}(T_a, G) = I_b\left[1 + \frac{\alpha_{Isc}}{100} \times (T_a - T_b)\right]\left(\frac{G}{G_b}\right) \quad (2)$$

Where:

T_a	Ambient temperature (deg C)
T_b	Base ambient temperature (deg C)
β_{Voc}	Arc current (amps)

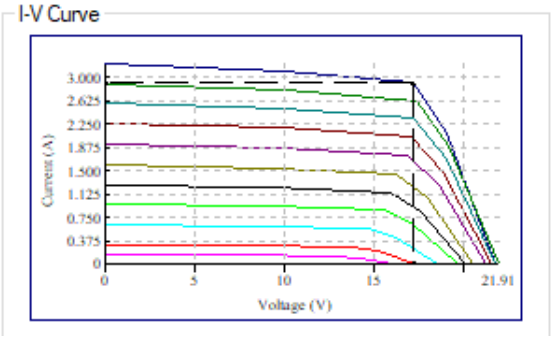

Fig. 2 Simplified Linear Estimation of Panel I-V curves

However, as the size of PV arrays and their voltage levels continue to increase, it might be possible that the arc voltage may shift to a more non-linear region of the I-V curves. Such condition may require the use of a more accurate mathematical representation of the I-V curves. This consideration may become more important under lower irradiance conditions. More accurate I-V curve estimation algorithms use single-diode and two-diode models. One of several examples for the I-V curves estimation process based on a single-diode model is described in [5].[6],[7] & [8]. A single-diode model is shown in Fig. 3.

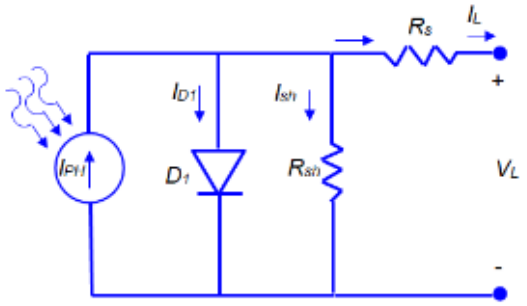

Fig. 3 Single-Diode Model for PV Cell

The number of parameters typically required to model an I-V curve includes several values which are not readily available. The current I_L and voltage V_L for a single-diode model can be represented using equations (3) and (4). There are several other versions and references to single-diode models, not included in this paper.

$$I_L = I_{ph} - I_o\left[exp\left(\frac{V_L + I_L \times R_s}{V_T}\right) - 1\right] - \frac{V_L + I_L \times R_s}{R_{sh}} \quad (3)$$

$$V_T = \frac{a \times N_s \times k \times T}{q} \quad (4)$$

Where:

I_{ph}	Photogenerated current (amps)
I_o	Diode reverse saturation current (amps)

R_S	Series Resistance (Ohms)
R_{sh}	Shunt Resistance (Ohms)
V_{T}	Thermal Voltage (volts)
V_{L}	Cell Voltage (volts)
a	Diode ideality factor
q	Electron charge (1.60217646x10^-19 C)
N_{S}	Series connected solar cells
k	Boltzmann constant (1.3806503x10^-23 J/K)
T	Working temperature (Kelvin)

The two-diode model is shown in Fig. 4, it introduces several new parameters as shown.

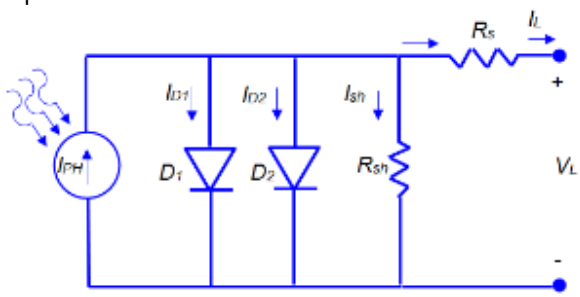

Fig. 4 - Two-Diode Model for PV Cell

An example of the characteristics and equations for a two-diode model are described in [9], [10] & [11] and several other resources. The I-V curves for a two-diode model can be obtained using equations (5) and (6). The mathematical representation of the panel using these equations requires the inclusion of two sets of diode parameters.

$$I_L = I_{ph} - I_{o1}\left[exp\left(\frac{V_L+I_LR_S}{V_{T_1}}\right)-1\right] - I_{o2}\left[exp\left(\frac{V_L+I_LR_S}{V_{T2}}\right)-1\right] - \frac{V_L+I_LR_S}{R_{sh}} \quad (5)$$

$$V_{T1} = \frac{a1\times N_S\times k\times T}{q}, \quad V_{T2} = \frac{a2\times N_S\times k\times T}{q} \quad (6)$$

Where:

I_{ph}	Photogenerated current (amps)
$I_{\mathrm{o1}}, I_{\mathrm{o2}}$	Diodes reverse saturation current (amps)
R_S	Series Resistance (Ohms)
R_{sh}	Shunt Resistance (Ohms)
$V_{\mathrm{T1}}, V_{\mathrm{T2}}$	Thermal Voltage (volts)
V_{L}	Cell Voltage (volts)
$a1, a2$	Diode ideality factor

The results of the estimation of the curves based on a single-diode or two-diode model provides two sets of I-V curves as shown in Fig. 5. In this figure, the simplified linear, single and two-diode curves are compared along with the PV module power output. The differences between the two estimations in this case only lead us to believe that the results of the dc arc-flash incident energy should increase proportionally with the increased accuracy of the two-diode model. The results of dc arc-flash simulations using the three approaches for modeling the I-V curves are presented later in this section.

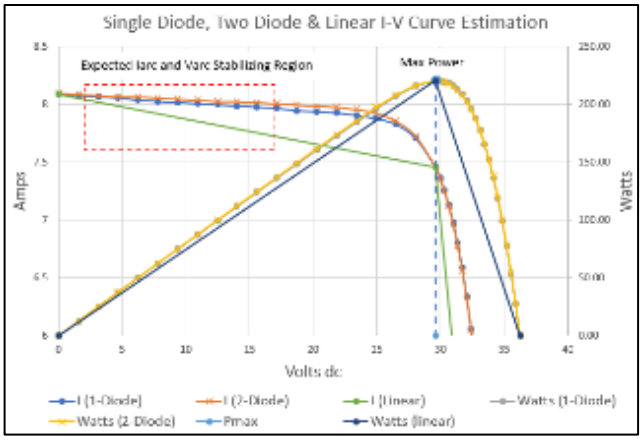

Fig. 5 - I-V Curve Estimation Model Comparison

Generally, the accuracy of the two-diode model is preferred to represent I-V curves of different PV manufacturers. The two-diode model is superior when subjected to irradiance and temperature variations. It exhibits excellent accuracy at lower irradiance conditions.

Now that the PV module and its I-V characteristics are modeled, the next step is to select the method to estimate the arc resistance and voltage. The process of integrating the I-V and arc characteristics into an iterative solution was first introduced to the electrical safety community in the form of a tutorial on arc-flash analysis for renewable energy systems presented at the 2105 ESW in Louisville KY [12]. In that tutorial, the preferred dc arc-flash method used is described in Ammerman [13]. Out of the methods mentioned in Ammerman, the preferred method to represent the dc arc resistance and voltage is the A.D. Stokes and W.T. Oppenlander method which is based on an exhaustive study of free-burning vertical and horizontal arcs between series electrodes in open air (see Fig. 6).

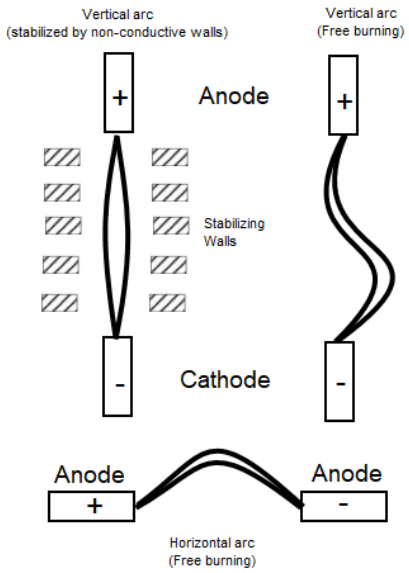

Fig. 6 - DC Arc Test Configurations

This model will be most accurate when used to simulate dc arcs in butted (series) electrode or conductor configurations. It

is less accurate for estimating the arc resistance and voltage for some configurations which are more likely to exist in equipment for PV installations and for configuration such as the ones used for this paper (See Fig. 7 - 9).

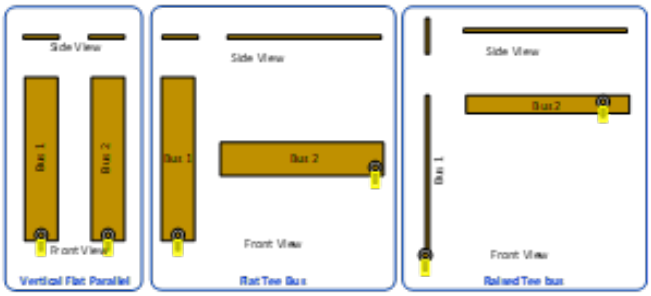

Fig. 7 - Bus Bar Test Configurations - Left to Right, Vertical Flat Parallel, Flat Tee, Raised Tee (NREL)

Fig. 8 - Vertical Flat Bus Configuration as tested (NREL)

Fig. 9 - Flat Tee Bus Bar Configuration as tested (NREL)

The "Stokes and Oppenlander" method arc resistance, voltage and current have been proposed for dc arcs. The arc resistance and voltage are determined based on equations (7) and (8). The model provides the arc voltage and current above the transition current. The transition current is the point at which the arc characteristic switches from high voltage vs. low current to low-voltage vs high current Eq (9).

$$R_{arc} = \frac{20+0.534\times Z_g}{I_{\text{arc}}{}^{0.88}} \quad (7)$$

$$V_{arc} = (20 + 0.534 \times Z_g) \times I_{\text{arc}}{}^{0.12} \quad (8)$$

$$I_T = 10 + 0.2 \times Z_g \quad (9)$$

Where:

R_{arc}	Arc resistance (Ohms)
V_{arc}	Arc voltage magnitude (volts dc)
I_{arc}	Arc current (amps)
Z_{g}	Gap between conductors (amps)
I_{T}	Transition current (amps)

The next step is to solve equations (7) and (8) to find the arc voltage and resistance including the proper short-circuit current effect of the PV modules. As mentioned during the introduction, one of the most important steps in the estimation of the incident energy for PV system is to include the effect of the I-V curves in the solution. This can be accomplished by using iterative solutions which include both the non-linear I-V curves and equations (7) and (8). Fig. 10 shows a simplified diagram showing the modules, the collector cables and a combiner box which can be used as an example to illustrate the solution process. The resistance of the cables R_c can be the equivalent combined cable resistance from the PV modules to the combiner.

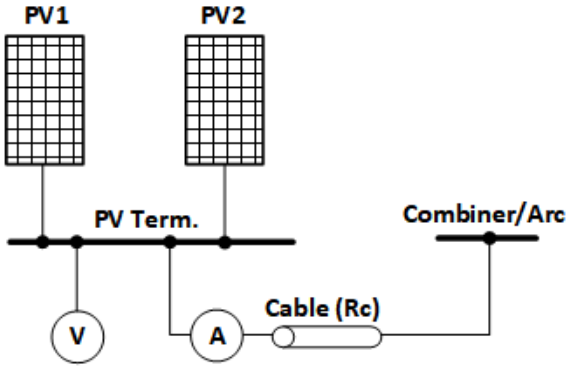

Fig. 10 - Arc Sensor Circuit (NREL)

The iterative routine can start by injecting the dc short-circuit current at the I_{sc} value of the modules and increase it using discrete steps until a solution is found. At every current step, the iterative solution updates the R_{arc} value estimated using the *Ibf* for the current step. An illustration of this process is depicted in Fig. 11. The solution criteria must satisfy both the Kirchhoff's Voltage Law closed loop circuit solution shown in Fig. 12 ($V_{PV\_Term} = V_{d\_Rc} + V_{arc}$) and the relationship between equations (7) and (8).

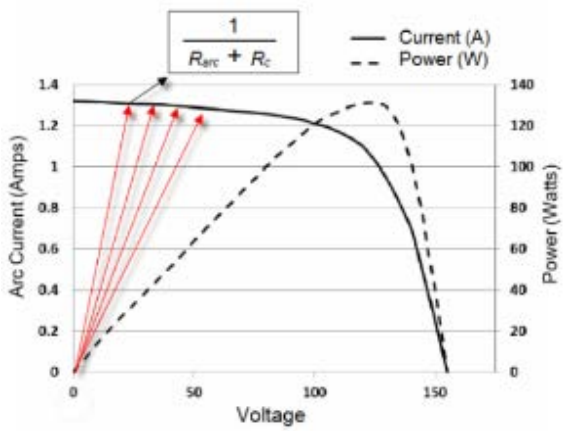

Fig. 11 – Illustration of Iteration Steps on I-V Curve

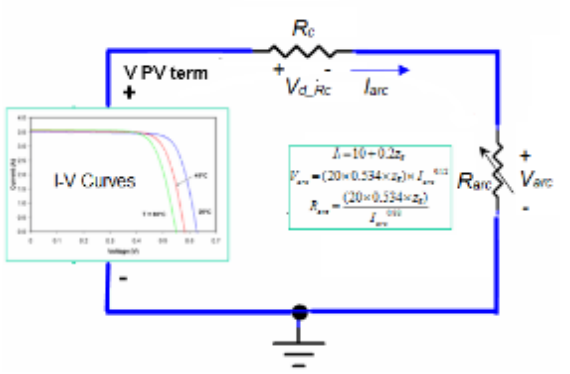

Fig. 12 – Illustration of Solution Criteria for V_{arc}, I_{arc} & R_{arc}

The next step is to determine the arc power and energy using equations (10) and (11) after having found the solution to (7) and (8).

$$P_{\text{arc}} = V_{\text{arc}} \times I_{\text{arc}} \quad (10)$$

$$\text{E}_{\text{arc}} = V_{\text{arc}} \times I_{\text{arc}} \times T_{\text{arc}} = {I_{\text{arc}}}^2 \times R_{\text{arc}} \quad (11)$$

Where:

T_{arc} Arc exposure duration in (seconds)

The incident energy can be determined using equations (12) and (13) developed based on [14] and applied in similar fashion as in [15] for various combinations of *a, k*, (which are functions of the box size and electrode orientation), and *x* (which is a function of gap and arc current magnitude).

$$E = \frac{E_{\text{arc}}}{4 \times \pi \times d^x} \quad (12)$$

$$E = k \times \frac{E_{\text{arc}}}{a^2 + d^x} \quad (13)$$

Where:

E Incident energy (Joules/cm^2)
E_{arc} Arc energy (Joules)
d Working distance (mm)
a Wilkins "a" reflectivity coefficient
k Wilkins "k" reflectivity coefficient
x Distance exponent coefficient

The "Stokes and Oppenlander" method is not well suited to calculating the arc resistance and voltage if the dc arc flash does not occur in a free-burning vertical or horizontal series electrode configuration (similar to that of the test shown in Fig. 8). Yet this approach agrees more closely with test results detailed later in this paper, Section VI. The difference between calculation and measured results is far less than what can be achieved using the methods proposed by [15], [16] and [17]. The lack of accuracy in determination of arc voltage and resistance is not a critical factor since the results of the "Stokes" method in combination with the "Wilkins" energy transfer method produce incident energy results which are higher than the majority of test results evaluated here and also by EPRI [18]. Section VI of this paper shows a comparative analysis and provides some potential adjustments to input parameters of the model to improve correlation with laboratory test results.

IV. DOUBLE ITERATIVE MODEL SIMULATIONS

The model described in Section III can be simulated using different software packages and commercially available power system analysis programs. Fig. 13 shows one potential implementation of the model using standard simulation blocks. The model includes the capability to use the linear, single-diode and two-diode I-V curves to calculate the dc arc-flash incident energy per the mathematical formulation in Section IV.

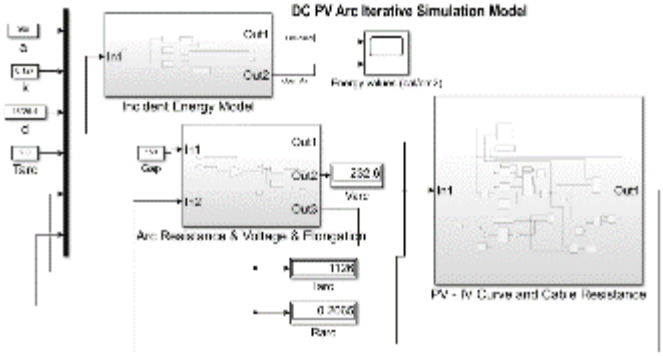

Fig. 13– dc AF in PV System Simulation Model

Three general case study or simulations were performed to observe the results of the model. A sample of the input parameter for two of these cases is provided in Table 1.

Table 1 - Input Parameter for Case 1 Simulation

Input Parameter	Case 1	Case 2	Unit
Voc	833	830	volts dc
Isc	1134	58.6	amps dc
Vmp	681	681	volts dc
Imp	1044	52.2	amps dc
Arc Duration	2.0	2.0	seconds
Gap	150	51	mm

A. Case 1: Comparison of PV I-V Curve Types

The double-iterative model was used to compute the incident energy of PV systems modeled using the three I-V curve representations discussed in Section III. The same input parameters were used while only varying the I-V curve model type. The results reveal that the increase in accuracy of the two-diode model results in a 2.7% increase in the incident energy as summarized in Table 2.

Table 2 - Comparison of I.E. for Different I-V Curve Types

I-V Curve Type	Incident Energy (cal./cm^2)
Linear	4.683
Single-Diode	4.770
Two-Diode	4.810

The difference could become higher since the output voltage and current of the PV systems continues to increase. Computer models should work fine with either the single or two-diode models for simulations.

B. Case 2: Model Result Comparison against experimental data

The model was also tested by comparing its output results against the test results described in Section III, Table 3.

Table 3 – Measured. vs. Calc. I.E. for NREL T-Flat Config. Test

Reflectivity Coefficients	Incident Energy (cal./cm^2)		% Diff.
	Measured	Calculated	
a = 100, k = 0.127	0.0414	0.087	71 %
a = 350, k = 0.127	0.0414	0.058	33 %

The model simulation results were compared against a T-flat configuration test. The result comparison shows a much smaller difference between measured and calculated incident energy than what is predicted by V_{mp} and I_{mp} methods. Based on previous findings of NREL and EPRI the difference between measured and calculated incident energy for V_{mp} and I_{mp} methods can be as high as 5 to 10 times.

A comprehensive set of comparisons of the double-iterative method to the lab test measurements is presented in Section VI.

C. Case 3: Model Result Comparison against EPRI Tests

The model was also tested by comparing its output results against the test results described in the EPRI report [18]. These tests had significantly higher arc current which drove the dc arc to behave more like a dc arc-flash. The test of [18] can cause a higher amount of convective heat transfer by the molecular cloud; however, the simulation results still show a good correlation with differences in the range of 5% to 70%.

D. Simulation of arc elongation

Based on the observations of the test results performed, it is apparent that the dc arcs experience a significant elongation effect. The elongation effect causes the arc column length to reach several inches and reach a peak arc voltage. Once the arc reaches a peak voltage, there is enough voltage build up across the conductor anode and cathode for a new arc to spark across a shorter path which is similar in length to the initial gap between conductors. The arc elongation effect depends on the available paths for the arc current to flow. Fig. 14 shows a plot of the effective arc column length for the same test shown in Fig. 15 and subsequent test data in Section V. The effective arc length was determined using (14) assuming the voltage drop on the anode and cathode were 23.1 volts and the voltage gradient was 34 volts/cm [12]. A further note, arc resistance was found to be directly proportional to the effective arc column length.

$$L_{arc}(t) = \frac{V_{\mathrm{arc}}(t) - V_{drop}}{V_G} \qquad (14)$$

Where:

V_{drop} Anode and cathode voltage drop (23.1 V)
$V_{\mathrm{arc}}(t)$ Total measured arc voltage (V)
V_{G} Voltage gradient (34 volts/inch)

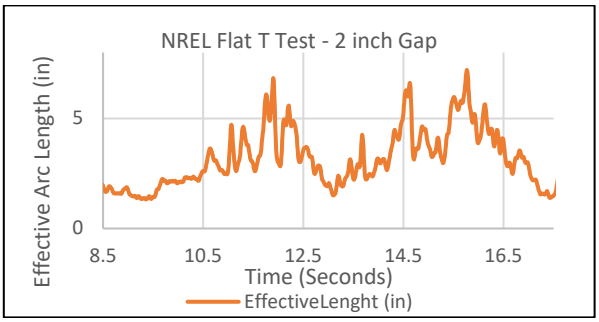

Fig. 14 – Arc Resistance and Length (for test from Fig. 7)

The average arc voltage was determined to be between 131 and 135 volts dc. The average arc resistance was estimated to be about 2.3 Ω. Using the proposed double-iterative model solving (7) and (8) along with the I-V curves, the arc voltage was determined to be 77 volts and the average arc resistance to be about 1.35 Ω. The arc voltage difference is significant since as shown in Fig. 15 the measured average arc voltage was 131.5 volts.

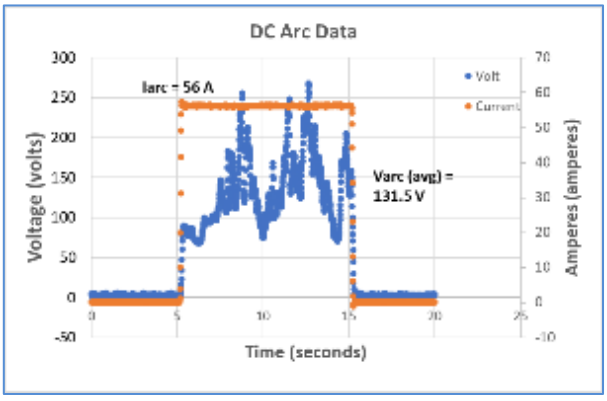

Fig. 15 - Typical Arc Test Plot - Voltage and Current as tested (NREL)

Fig. 16 shows a snapshot of the arc elongation experienced during the arcing time. The effective arc length is several inches..

Fig. 16 – Flat Tee Bus arc test showing arc elongation between bus bars (NREL)

The arc elongation effect can account for several arc elongation functions. One method as described in [19] and [20] can account for arc elongation as a function of time. The effect of the arc elongation is represented using (15) and (16):

$$R_{arc}(t) = R_{arc0}(t)\left[1 + \alpha e^{\beta(t-T_i)}\,\mathrm{h}(t-T_i)\right] \quad (15)$$

$$V_{arc}(t) = V_{arc0}(t)\left[1 + \alpha e^{\beta(t-T_i)}\,\mathrm{h}(t-T_i)\right] \quad (16)$$

Where:

$R_{\mathrm{arc}}(t)$	Average arc resistance vs time (Ω)
$V_{\mathrm{arc}}(t)$	Average arc voltage vs time (Ω)
$R_{\mathrm{arc0}}(t)$	Initial average arc resistance from (7) (Ω)
$V_{\mathrm{arc0}}(t)$	Initial average arc voltage from (8) (volts)
α	Proportional arc elongation coefficient
β	Exponential arc elongation coefficient
T_{i}	Inception or arc ignition time (sec)
h*(t)*	Heaviside function

Using (15) and (16) in the proposed model for double iteration between the arc characteristics and the I-V curves, the average arc resistance for a two-second duration arc was found to be about 135.17 volts and the arc resistance was found to be about 2.413 Ω. These results were obtained solving (15) and (16) using α = 0.025, β = 0.75, T_i = 25 ms and the standard Heaviside function. The arc duration of two (2.0) seconds is an industry standard arc maximum duration for most incident energy calculations. The solution of the arc elongation effect presented in (15) and (16) may be solved up to this arc duration.

The proposed model of [16] for incident energy seems to yield higher incident energy reflection than what has been observed in experimental data. This is very likely since it was developed to match the incident energy reflectivity of higher arc energy events with arc currents about 10 times or higher than what has been tested for dc PV tests. The effect of ionization and molecular cloud convective heat transfer is higher as the current increases. The standard a and k coefficients from [14] for different enclosure sizes yield conservative results; however, there is room for improvement in the selection of this thermal reflectivity coefficients. The authors used the proposed iterative model to test alternative values of a and k which still yield conservative results but reduce the overall extra conservatism from 100% (or higher) in most cases to less than 25 to 50%. Section VI presents the results of the comparative analysis of the results from laboratory testing and EPRI's data [18] using the adjusted a and k coefficients but without using the arc elongation effects. Overall, the standard size a and k coefficients may be fine for general use considering the overly conservative results provided by other methods such as [5], [12] and [17].

V. Laboratory Testing

Lab and field measurements were collected to validate incident energy models for PV systems and further expand on previously reported data [21]. An experimental mockup was developed comprising a source of PV energy, a set of electrodes for arc generation, and energy sensing equipment including voltage and current sensing, and copper calorimeter plates (Fig. 1). High-speed current and voltage measurements are collected with a data acquisition board operating at 250 samples per second which included high voltage isolation between channels. Current sensing is accomplished with a resistive 100 ampere, 50 milli-volt output current shunt, and voltage sensing with a precision 1000 to 1 voltage divider. Uncertainty for voltage channel was calculated to be +/-0.25%, current channel was +/-0.25%. Temperature channels used were K-type thermocouple and were verified before testing as repeatable within +/-0.5 deg. C.

Arcing energies were measured using copper-slug calorimeters constructed following American Society for Testing and Materials (ASTM(E457) [22] and F1959/F1958/M [23] standards. Two types of copper slugs were used, weighing in at 9 and 18-grams respectively. When initial test data was analyzed, it was found that temperature rise and response times were low for the 10kW and 30kW PV systems using the 18-gram calorimeters so the 9-gram calorimeters were fabricated. In several tests, the 9-gram units were found to be inconsistent and were excluded from the final dataset, but voltage and current data was useful in modeling validation. Where the 9-gram calorimeter data was found to be accurate, these lighter sensors provided better resolution and improved response to the low energy tests. Verification of calorimeters was performed by exposing the sensors to a 500-watt halogen lamp for a few seconds and recording the calorimeter temperature rise.

To generate DC arcs approximating real world conditions, several commercially available combiner boxes were examined to find common bus configurations. Based on these examples, the following configurations were chosen; vertical flat parallel, flat tee and raised tee, shown in Fig. 7 - 9. Electrodes were made of copper (Cu 110) bars measuring 6 inches long, 1 inch wide and 1/8 inch thick. Several test arcs were generated at each configuration to verify data accuracy and repeatability.

Bus bars were electrically isolated from the enclosure and mounted to the backplane using insulating standoffs, rated for 2500 V. The enclosure used was a standard National Electrical Manufacturers Association (NEMA) 12, 20 inch x 20 inch x 20 inch painted steel. Buses were mounted to a 19 inch by 19 inch standard painted steel backplane, See Figs. 8 and 9. The same enclosure and back plane were used for the entire

testing cycle. Calorimeter sensors were spaced 18 inches (45.72 cm) from the bus bars.

The energy for DC arc generation was supplied by a PV system, consisting of six strings of 23 or 24 modules. Each string generated just over 900 VDC open circuit and averaged around 9 amps short circuit current. The six strings were connected in parallel to provide an equivalent 35 kW DC photovoltaic system. Test voltage and current curves (IV curves) were taken to verify maximum power levels after each test run.

Each test run was performed using the following steps: DC disconnects were opened, zero energy verified, bus bars were cleaned then electrically connected with 4-8 turns of sacrificial 32 AWG solid magnet wire to create an initial arc path. Next a continuity verification between bars was performed, DC disconnects were closed, data collection was started, imaging was started, and finally the automated contactor system was engaged, starting the flow of DC current. Data were recorded for a few seconds before, during the ten second contactor closure, during the XX to YY seconds of active arcing, and a few seconds after the arc was extinguished. As current flowed, the sacrificial wire heated up and eventually vaporized and ignited an arc. After each arc event, the PV strings were isolated, and a timestamped I-V curve was taken. About 100 arcs were initiated and evaluated to present the 30 datasets in this paper. Any inconsistent or noisy data, or arcs lasting less than 5 seconds were also excluded.

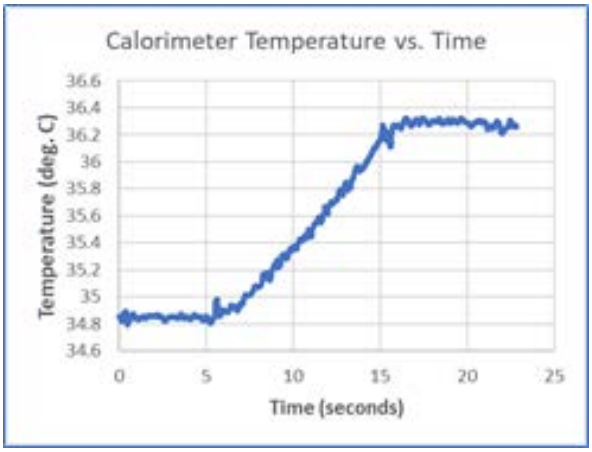

Fig. 17 - Calorimeter Data - Showing Temp. Rise

Typically, useful arc tests show a calorimeter response similar to Fig. 17 and voltage and current response as in Fig. 15. Depending on arc durations and bus configurations, the thermal response of the calorimeter directly corresponds to the incident energy as indicated in ASTM/E457-08.

When measured current and voltage data from an arc test are overlaid with the corresponding PV system's I-V curve, it becomes apparent that arcing events operate at a much lower voltage than normal operating or maximum power points of the PV system (Fig. 18). This may provide needed improvements to NFPA's annex D model for DC incident energy [1]. Looking at the I-V curve in Fig 18, PV system maximum power under normal operating conditions is 26.7 kW, while average arcing power observed during this test was 3.7 kW —a value 7 times lower. The discrepancy between PV power available and arc power practically generated is directly attributed to the voltage of the arc, which is itself determined by arc resistance and arc distance, both of which can vary depending on the bus geometry and environmental conditions.

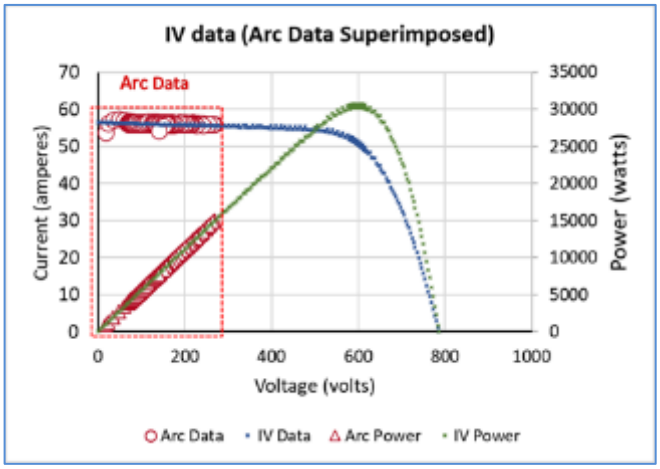

Fig. 18 - Typical Arc Test Data Plotted with IV Data for PV Strings - as tested (NREL)

Some general conclusions can be drawn on the impact of bus configuration on voltage and incident energy: maximum voltages observed during arcing were roughly 20-60% of open circuit PV voltage (Fig. 19 & Table 4); average arc voltages observed were 10-40% of the IV maximum power voltage (Fig. 19 & Table 5); and maximum current values during arcing almost equal the I-V short circuit current found in the I-V curve (Figs. 15 and 18).

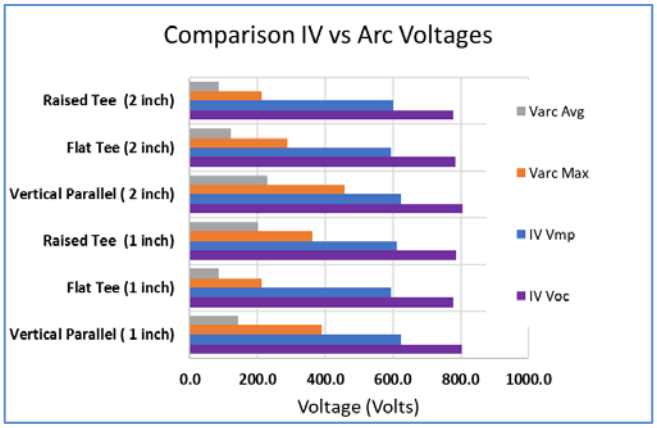

Fig. 19 – Average Voltage Data for each Bus Configuration (NREL)

Data in Fig. 18 show the comparison between the I-V or expected voltage and arc voltages. There are clear differences in the two data sets and differences in the bus configurations. Looking at the limited data, it appears that bus configurations in a tee configuration generate lower voltages during arcing than the parallel buses. This observation needs more study before it can be accepted as fact.

Table 4 – Average Maximum PV Voltage Data – IV Voc vs Arc (NREL)

Test (Arc Distance)	IV Voc	Varc Max	Ratio (V_{arc}/V_{IV})
Vertical Parallel (1 inch)	804.1	389.4	0.5
Flat Tee (1 inch)	778.7	212.6	0.3
Raised Tee (1 inch)	786.1	362.3	0.5
Vertical Parallel (2 inch)	805.0	456.3	0.6
Flat Tee (2 inch)	783.3	287.9	0.4
Raised Tee (2 inch)	778.7	212.6	0.3

Table 5 - Average PV Voltage – IV Vmp vs Arc (NREL)

Test (Arc Distance)	IV Vmp	Varc Avg	Ratio (V_{arc}/V_{IV})
Vertical Parallel (1 inch)	622.9	143.6	0.2
Flat Tee (1 inch)	594.6	85.2	0.1
Raised Tee (1 inch)	611.2	201.6	0.3
Vertical Parallel (2 inch)	624.5	230.4	0.4
Flat Tee (2 inch)	594.7	121.2	0.2
Raised Tee (2 inch)	600.0	85.2	0.1

Combining data for all test runs and separating by arc distance, it appears, as expected, that larger arc gaps generate higher incident energy, Fig. 20. Note, the average incident energies in both data sets are lower than the 500-watt halogen calibration test lamp at 12 inches (30.48 cm), 0.06 watts/cm^2. Note, these results are specific to current testing as larger commercial PV systems will have proportionally higher incident energy.

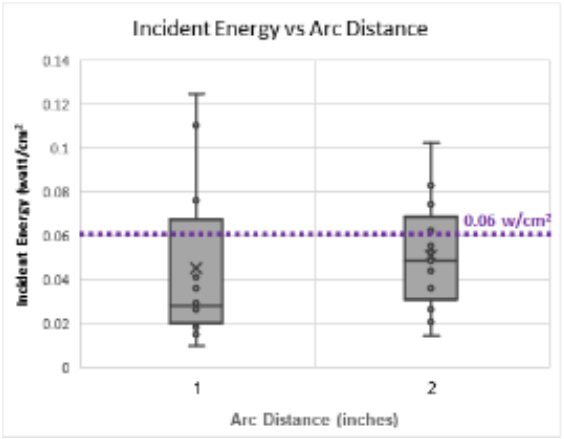

Fig. 20 – Arc Incident Energy vs Arc Distance, with 500-watt calibration lamp energy line at 0.06 watt/cm^2 (NREL)

VI. COMPARATIVE ANALYSIS RESULTS

This section provides a summary of the comparisons between measured test results and simulation results. Fig. 21 and Fig. 22 show the comparisons against test runs from Section V, Fig. 21 shows the comparison using the a and k coefficients for T-Flat configuration. Fig. 22 shows the same for a vertical parallel conductor arrangement. The results of the T configurations show overall better agreement with the simulation since the T configuration tests showed overall less arc elongation and thus the predicted arc resistance and voltage of (7) and (8) are closer than predicted for the vertical parallel configuration which showed higher arc elongation effects. Figs. 23 and 24 show the same comparisons but using a = 350 and k = 0.127 reflectivity coefficients. Observation of the comparisons indicates that test number 9 is likely an error in the measurement of the small incident energy since all remaining tests are less than simulated values. Furthermore, the tests compared in Figs. 21 to 24 do not have sufficient ionization energy to cause significant convective and conductive heat transfer, so the energy measured is mainly due to radiation. Observation of Figs. 23 and 24 shows that the simulation results obtained with a = 350 and k = 0.127 are less conservative; however use of these reflectivity coefficients improves the model simulation accuracy for comparisons against the tests of [18]. Since the arc currents and ionization energy of the tests of [18] are higher, better correlation against these test results is more important.

Comparison results against the test results of [18] are provided in Figs. 25, 26 and 27. The simulation results were generated using a = 350 and k = 0.127 reflectivity coefficients. As noted earlier, the correlation against the measured test results significantly improves using these coefficients.

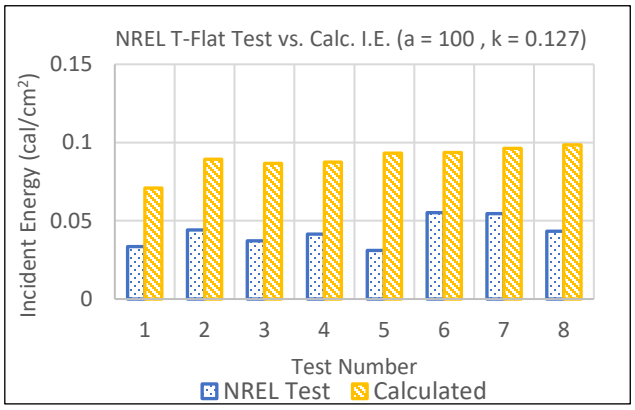

Fig. 21 – Lab Meas. vs Calc. I.E (T-Config)

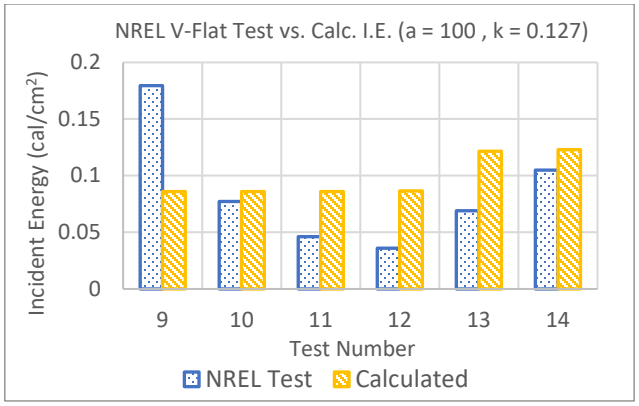

Fig. 22 – NREL Lab Meas. vs Calc. I.E (V Parallel-Config)

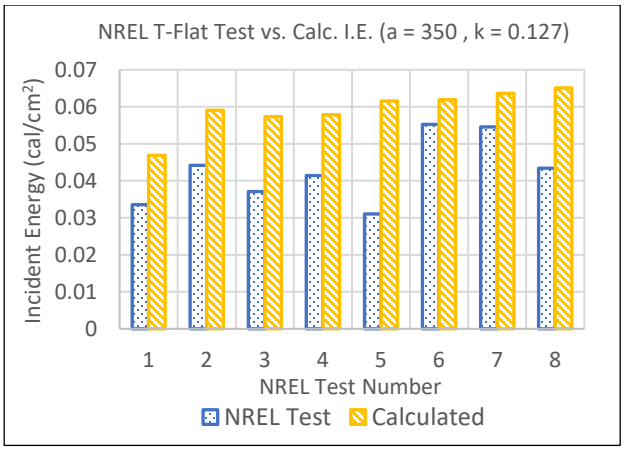

Fig. 23 – Lab Meas. vs Calc. I.E (T-Config). Rev. a, k.

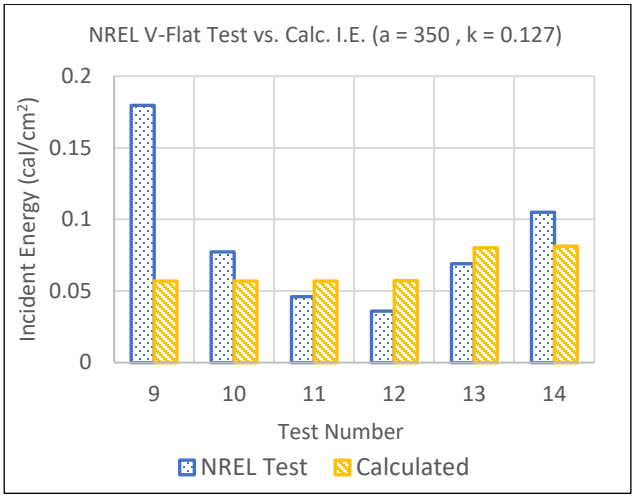

Fig. 24 – Lab Meas. vs Calc. I.E (V Parallel-Config). Rev a, k.

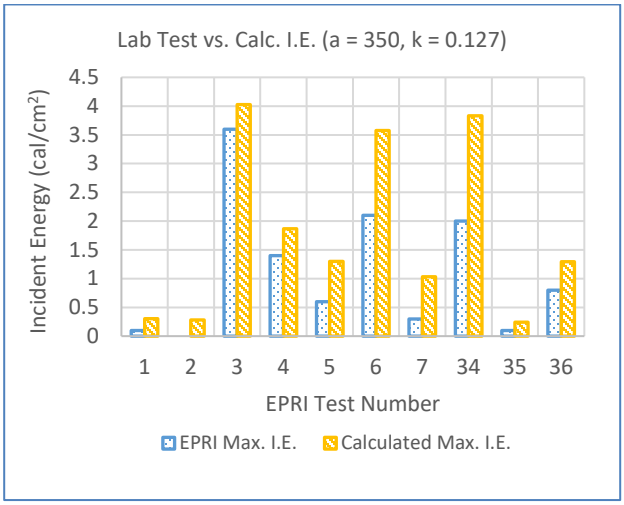

Fig. 25 – EPRI Test Meas. vs Calc. I.E. Rev. a, k.

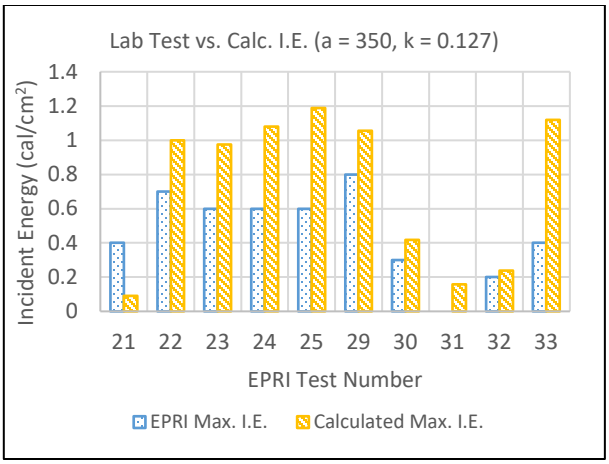

Fig. 26 – EPRI Test Meas. vs Calc. I.E. Rev. a, k.

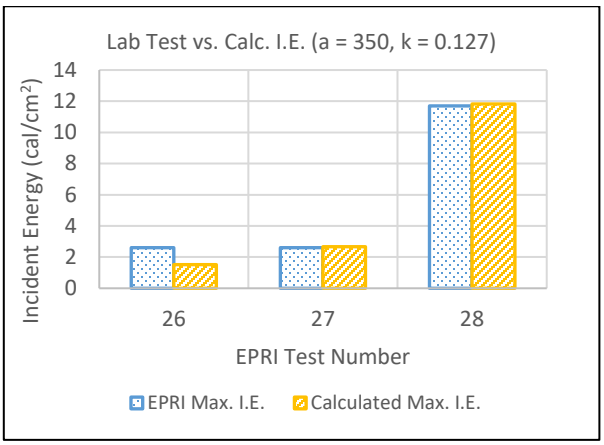

Fig. 27 – EPRI Test Meas. vs Calc. I.E. Rev. a, k.

The comparative analysis results presented in this section do not include the arc elongation effects described in Section IV; however, if it is included, it should reduce the differences between simulation and measurements. The only comparison against test results which included this elongation effect is for the test shown in Figs. 14, 15 and 16. Future work should focus on how much arc elongation can occur under different electrode configurations.

VII. PPE CONSIDERATIONS

It is not the intent of this paper to present a method to select personal protective equipment (PPE) or to make recommendations on how it should be used. The purpose of arc-flash PPE is to minimize burn injuries by providing a thermal barrier that will limit the energy exposure to a worker's skin to an incident energy below 1.2 cal./cm^2 (generally considered the onset of a second -degree burn) when working inside the arc-flash boundary. Generally, the most popular calculation methods such as those described in [15],[16],[17] tend to overestimate the incident energy and consequently result in higher arc thermal performance value (ATPV) and break-open threshold (EBT) PPE ratings required for an energized equipment task. However, the heavier and bulkier PPE selection may lead to other hazards such as heat exhaustion or accidental contact with energized conductors.

According to Gordon et al, in [24] not a single documented injury or fatality was found from a DC arc flash lower than 500 V DC when reviewing the OSHA database from 1984 to 2018. Of 120 incidents of death from arc flash, only 2 were in DC systems, both above 500 Vdc. One being a metal production facility with high power electrolytic cell lines, the other being a 500 V battery bank. The dc short-circuit current in such equipment is generally considered to be an order of magnitude higher than what is available in most PV array systems.

PV Systems are different than other types of dc systems e.g., Capacitors, Transit Systems, Batteries, etc. Workers should be appropriately protected from the hazards associated with the type of DC system they are working on. Recently the trend in IEEE research publications such as EPRI [18] and Sekulic [19] measured results were much lower compared to the maximum power model results - by a factor of 5 to 10 times. The biggest goal of this paper and others is to provide more refined incident energy calculation methods to more accurately quantify the PPE selection for PV systems to reduce hazards possibly introduced by heavier PPE use.

VIII. CONCLUSIONS

The results of the tests performed by NREL are one more step in the evolution test data needed to validate dc arc-flash models in PV systems. Many more tests are needed for the development of the models, and hopefully this work along with others to come will pave the way for the development of a standard for dc arc-flash incident energy analysis similar to [25]. Eventually such standards will be a valuable part of [1].

It can be concluded that future models will need to consider electrode configurations or conductor orientations like those presented in [25] but experimentally determined to align with dc PV equipment configurations. The “Stokes and Oppenlander” method is adequate to determine the arc resistance voltage and current for vertical or horizontal series electrodes but falls short when estimating the results of vertical parallel conductors (V-Configuration) or perpendicular conductors (T-Configuration).

It can also be concluded that the “Stokes and Oppenlander” method can be used as a starting point to estimate the initial arc voltage and resistance and that it could be adjusted based on potential arc elongation functions to estimate a more accurate average arc voltage and resistance values. More research is needed to be able to conservatively estimate the arc elongation effect, but the authors feel that the method presented here are a step in the right direction.

It can be concluded as well that the more accurate double-diode model to represent the I-V curves provides the most accurate and conservative arc power results but that single diode and linear models provide fairly accurate results with no more than a 5% difference. The double iteration process between the I-V and dc arc equations provides accurate yet conservative results and as previously mentioned brings a more accurate representation of the PV system short-circuit current which is one of the most important aspects to accurately estimate the dc arc flash operational characteristics which are far from the maximum power delivery point of the dc PV modules. Future models will also need to include different electrode configurations which the authors consider essential to represent dc arcs in actual combiner and inverter enclosures.

IX. ACKNOWLEDGEMENTS

The authors thank the following people for their help and support with this paper: Heath Garrison, Gregory Martin, Teresa Barnes, Ingrid Repins, Byron McDanold and Josh Parker. The authors would also like to acknowledge the valuable support of Dr. Farrokh Shokooh. This work was authored in part by Alliance for Sustainable Energy, LLC, the manager and operator of the National Renewable Energy Laboratory for the U.S. Department of Energy (DOE) under Contract No. DE-AC36-08GO28308. Funding provided by the U.S. Department of Energy Office of Energy Efficiency and Renewable Energy (EERE) Solar Energy Technologies Office (SETO). The views expressed in the article do not necessarily represent the views of the DOE or the U.S. Government. The U.S. Government and the publisher, by accepting the article for publication, acknowledges that the U.S. Government retains a nonexclusive, paid-up, irrevocable, worldwide license to publish or reproduce the published form of this work, or allow others to do so, for U.S. Government purposes

X. REFERENCES

[1] NFPA 70E, 2021 *Standard for Electrical Safety in the Workplace*, Quincy MA: NFPA

[2] NFPA 70, 2020 *National Electric Code*, Quincy MA: NFPA

[3] 1910.33, Occupational Safety and Health Administration Requirements: United States Department of Labor.

[4] P. McNutt, W. R. Sekulic and G. Dreifuerst, "Solar/Photovoltaic DC Systems: Basics and Safety," 2018 *IEEE IAS Electrical Safety Workshop (ESW)*, Fort Worth, TX, USA, 2018, pp. 1-9, doi: 10.1109/ESW41044.2018.9063869.

[5] Dobos, A, “An Improved Coefficient Calculator for the California Energy Commission 6 Parameter Photovoltaic Module Model,” 2012 in Journal of Solar Energy Engineering, Vol 34, pp. 2-6, doi: 10.1115/1.4005759

[6] De Soto, W, “Improvement and Validation of a Model for Photovoltaic Array Performance,” 2004 Thesis in Solar Energy Laboratory of Wisconsin-Madison 2004

[7] Hussein, A., “A simple Approach to extract the unknown Parameters of PV modules,” 2017 Turkish Journal of Electrical Engineering & Computer Sciences, pp. 4431-4432, doi: 10.3906/elk-1703-14

[8] IEC Standard 60891:2009, “Photovoltaic devices – Procedures for temperature and irradiance corrections to measured I-V characteristics.”

[9] AlRashidi, R., et al, “Parameters Estimation of Double Diode Solar Cell Model,” 2013 World Academy of Science, Engineering and Technology International Journal of Electrical and Computer Engineering, Vol: 7, No:2

[10] A. J. Nascimento, M. C. Cavalcanti, F. Bradaschia, E. A. Silva, L. Michels and L. P. Pietta, "Parameter estimation technique for double-diode model of photovoltaic modules," 2017 Brazilian Power Electronics Conference (COBEP), Juiz de Fora, 2017, pp. 1-6, doi: 10.1109/COBEP.2017.8257242.

[11] Ishaque, K, et al, “Simple, fast and accurate two-diode model for photovoltaic modules,” 2010 in Solar Energy

Materials & Solar Cells, www.elsevier.com/locate/solmat, pp. 588-589
[12] K. Klement, "DC arc flash studies for solar photovoltaic systems, challenges and recommendations," 2015 *IEEE IAS Electrical Safety Workshop*, Louisville, KY, 2015, pp. 1-4, doi: 10.1109/ESW.2015.7094947
[13] R. F. Ammerman, T. Gammon, P. K. Sen and J. P. Nelson, "Dc arc models and incident energy calculations," *2009 Record of Conference Papers - Industry Applications Society 56th Annual Petroleum and Chemical Industry Conference*, Anaheim, CA, 2009, pp. 1-13, doi: 10.1109/PCICON.2009.5297174.
[14] R. Wilkins, "Simple Improved Equations for Arc Flash Hazard Analysis", August 30, 2004. Online at IEEE Electrical Safety Forum
[15] A. Marroquin, A. Rehman and A. Madani, "High-Voltage Arc Flash Assessment and Applications," in IEEE Transactions on Industry Applications, vol. 56, no. 3, pp. 2205-2215, May-June 2020, doi: 10.1109/TIA.2020.2980467.
[16] D. R. Doan and R. M. Derer, "Arc flash calculations for a 1.3 MW photovoltaic system," presented at the IEEE IAS Electrical Safety Workshop, San Diego, CA, USA, Paper ESW2014-03
[17] E. H. Enrique et al., "DC arc flash calculations for solar farms," in Proc. 1st IEEE Conf. SusTech, 2013, pp 97–102
[18] EPRI, "DC Arc Flash on Photovoltaic Equipment," June 2018 Technical Report, 3002014124
[19] V. Terzija, G. Preston, M. Popov and N. Terzija, "New Static "AirArc" EMTP Model of Long Arc in Free Air," in *IEEE Transactions on Power Delivery*, vol. 26, no. 3, pp. 1344-1353, July 2011, doi: 10.1109/TPWRD.2010.2086082
[20] V. V. Terzija and H. -. Koglin, "New approach to arc resistance calculation," 2001 *IEEE Power Engineering Society Winter Meeting. Conference Proceedings (Cat. No.01CH37194)*, Columbus, OH, USA, 2001, pp. 781-787 vol.2, doi: 10.1109/PESW.2001.916958.
[21] W. R. Sekulic and P. McNutt, "Evaluating the Incident Energy of Arcs in Photovoltaic DC Systems: Comparison Between Calculated and Experimental Data," in *IEEE Transactions on Industry Applications*, vol. 56, no. 3, pp. 3224-3230, May-June 2020, doi: 10.1109/TIA.2020.2980217.
[22] ASTM/E457-08, "Standard Test Method for Measuring Heat-Transfer Rate Using a Thermal Capacitance (Slug) Calorimeter," Reapproved 20
[23] ASTM/F1959/F1959 – 14, "Standard Test Method for Determining the Arc Rating of Materials for Clothing," January 2017.
[24] L. B. Gordon, et al., "Electrical Injuries and Fatalities: Facts, Myths, and Unknowns", IEEE ESW 2019-32
[25] D. Mohla, W. Lee, J. Phillips and A. Marroquin, "Introduction to IEEE Standard. 1584 IEEE Guide for Performing Arc-Flash Hazard Calculations- 2018 Edition," 2019 *IEEE Petroleum and Chemical Industry Committee Conference (PCIC)*, Vancouver, BC, Canada, 2019, pp. 1-12, doi: 10.1109/PCIC30934.2019.9074501

XI. VITA

William Sekulic, BSEE, PE, PV Reliability Group at National Renewable Energy Laboratory, Golden, Co. since 2001. His research areas include photovoltaic reliability, battery storage, balance of systems components and electrical safety. He is also a member of the electrical safety committee and part time electrical inspector. He graduated from Colorado School of Mines and is a professional engineer registered in the state of Colorado.

Albert Marroquin, BSEE, PE – V.P., Electrical Safety & Dynamics Eng. Divisions, Senior Principal Electrical Engineer – ETAP. Mr. Marroquin is a registered professional engineer in the state of California. He is also the main designer and product manager for ETAP's AC and DC Arc Flash products as well as a working group member of IEEE 1584. Albert has over 20 years of experience in the development of advanced engineering mathematical algorithms and software development.

Peter McNutt graduated from the University of Colorado at Denver in 1994 with an MSEE. He began working at NREL in 1997 in the areas of PV performance, deployment, and energy systems integration. In the Energy Systems Integration Facility at NREL part of his time is spent as an electrical safety officer performing electrical safety inspections and updating arc-flash hazard analyses for AC and DC equipment. He is a registered professional engineer in the State of Colorado.